Carrier Lifetime Degradation and Regeneration in Gallium- and Boron-Doped Monocrystalline Silicon Materials

Michael Winter, Dominic C. Walter, and Jan Schmidt

***Abstract*—In this article, carrier lifetime degradation phenomena on fired gallium-doped Czochralski-grown silicon (Cz-Si:Ga) and boron-doped float-zone silicon (FZ-Si:B) are observed. We examine lifetime degradation and regeneration as a function of illumination intensity and temperature and observe qualitatively similar degradation effects in both material classes, which are triggered by a fast-firing high-temperature step. Charge carrier injection, e.g., through illumination, is required to activate the defects responsible for degradation. The extent of degradation increases with increasing temperature, which is untypical for degradation effects reported before. Despite different degradation time constants are measured for Cz-Si:Ga and FZ-Si:B, the activation energies are for both materials in the narrow range (0.58 ± 0.04) eV. The extracted activation energy is quite different compared with other degradation effects in silicon, suggesting a novel defect formation mechanism. Since the lifetime degradation is triggered by the fast-firing of the silicon wafers during the presence of a hydrogen-rich dielectric at the surface, the involvement of hydrogen in the defect reaction is very likely. During prolonged illumination at elevated temperature (135 °C), we observe a permanent regeneration of the lifetime, whereas at temperatures close to room temperature (36 °C), the defect deactivation is only temporary.**

***Index Terms*—Carrier lifetime, degradation, gallium, Light-Induced Degradation (LID), regeneration, silicon (Si).**

I. Introduction

LIGHT-INDUCED lifetime degradation effects are frequently observed in crystalline silicon materials for solar cell production. One of the most prominent ones is caused by the electron-induced activation of a boron-oxygen (BO) defect, which is typically occurring in boron-doped Czochralski-grown silicon (Cz-Si) [1]–[4]. Another degradation effect is the so called *light and elevated temperature-induced degradation* first observed on block-cast multicrystalline silicon (mc-Si) [5]–[7]. In contrast to the BO-related degradation effect, the occurrence of the LeTID effect requires a previous fast-firing step at a high peak temperature [8]–[10]. There have been reports of LeTID-type effects in boron-doped Cz-Si [11]–[13], in float-zone silicon (FZ-Si) and in *n*-type Cz-Si [14]–[16]. More recently, lifetime instabilities on gallium-doped Cz-Si wafers and solar cells have been reported, too [17]–[19]. Whether these degradation effects have the same physical root cause as LeTID on mc-Si remains a question of ongoing debates [20], [21]. In this study, we perform a series of carrier lifetime experiments to examine degradation effects in gallium-doped Cz-Si (Cz-Si:Ga), which is increasingly applied in industrial solar cell production because of the absence of BO-related degradation. As a reference, we also study boron-doped float-zone silicon (FZ-Si:B), as the most defect-lean silicon material available today. Both materials are, for different reasons (no B-doping in case of Cz-Si:Ga, a very low oxygen contamination in FZ-Si:B), not prone to BO degradation and are therefore excellent test subjects for detailed degradation experiments.

II. Experimental Details

Symmetrical lifetime samples are processed on 1 Ω cm-Cz-Si:Ga and 1.2 Ω cm-FZ-Si:B wafers. The saw damage of the wafers is removed in a KOH solution before cleaning them in a standard RCA sequence. Then, a double-sided phosphorus diffusion is performed in a quartz-tube furnace at a process temperature of 829 °C. The resulting phosphosilicate glass and the n^+-layers of ∼47 Ω/sq on both wafer surfaces are removed by an HF dip and a KOH solution. After another RCA cleaning, both wafer surfaces are symmetrically coated with Al_2O_3/SiN_x stacks. First, 10 nm of aluminum oxide (Al_2O_3) is deposited by plasma-assisted atomic layer deposition (Oxford Instruments, FlexAL). Subsequently, 100 nm of silicon nitride (SiN_x) with a refractive index of $n = 2.05$ is deposited on top by plasma-enhanced chemical vapor deposition (Meyer Burger, SiNA). As a reference, some wafers are annealed at 425 °C for 15 min to activate the surface passivation without a fast-firing step. The remaining wafers receive a firing treatment in an industrial conveyor-belt furnace (centrotherm international, DO-FF-8.600-300) at a set-peak temperature of 850 °C and a belt speed of 6.8 m/min, resulting in a measured peak temperature of (750 ± 10) °C for the Cz-Si:Ga wafers and (710 ± 10) °C for the FZ-Si:B wafers. The wafer temperatures were measured using a temperature tracker (Datapaq DQ1860A) and a type-K

Manuscript received January 26, 2021; revised March 12, 2021; accepted March 30, 2021. This work was supported in part by the German State of Lower Saxony and in part by the German Federal Ministry for Economic Affairs and Energy within the research project LIMES (contract 0324204D) *(Corresponding author: Michael Winter.)*

Michael Winter and Jan Schmidt are with the Institute for Solar Energy Research Hamelin/Emmerthal (ISFH), 31860 Emmerthal, Germany, and also with the Institute of Solid-State Physics, Leibniz University Hannover, 30167 Hannover, Germany (e-mail: m.winter@isfh.de; j.schmidt@isfh.de).

Dominic C. Walter is with the Institute for Solar Energy Research Hamelin/Emmerthal (ISFH), 31860 Emmerthal, Germany (e-mail: d.walter@isfh.de).

Color versions of one or more figures in this article are available at https://doi.org/10.1109/JPHOTOV.2021.3070474.

Digital Object Identifier 10.1109/JPHOTOV.2021.3070474

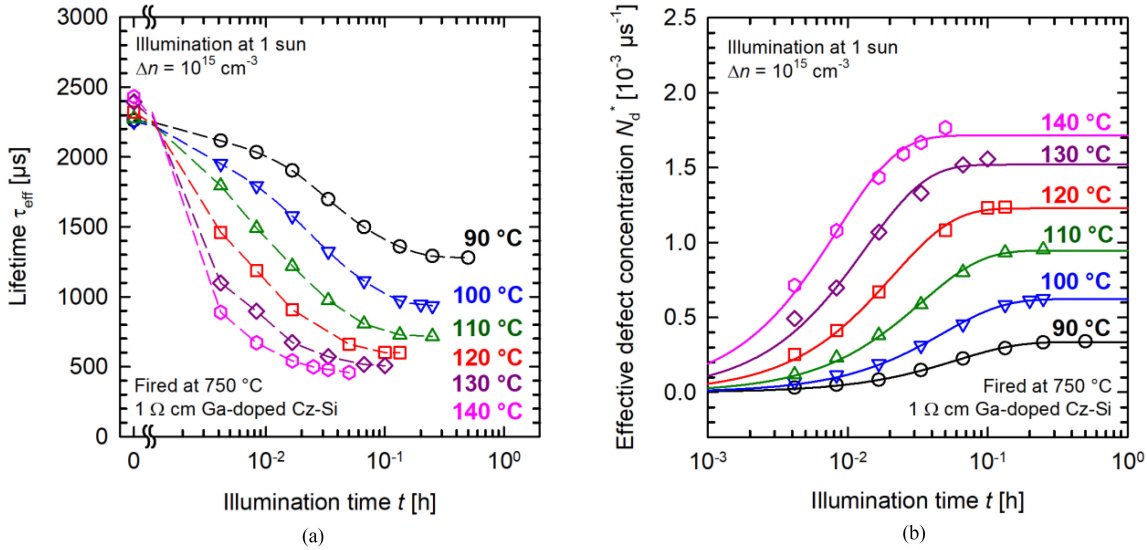

Fig. 1. Lifetime degradation of Cz-Si:Ga illuminated at 1 sun at temperatures ranging from 90 to 140 °C. (a) Effective lifetime τ_{eff} at $\Delta n = 10^{15}$ cm^{-3}, as a function of illumination time t. The dotted lines serve as guide to the eye. (b) Corresponding effective defect concentration $N_{\text{d}}^{*}(t)$ [colors and symbols match the graphs in (a)]. The lines are exponential rise-to-maximum fits of the measurement data calculated by using (2).

thermocouple (Omega, KMQXL-IM050G-300). After firing, the wafers are cut into 5 × 5 cm samples using a laser process. The final thickness of all samples is (150 ± 10) μm.

After finishing the processing, the samples receive the following treatment: Halogen lamp illumination on a hotplate at elevated temperatures between 70 and 140 °C with illumination intensities ranging from 0.1 to 1 sun until the degraded state is reached (i.e., the defect is fully activated). We measure the illumination intensity with a calibrated reference silicon solar cell. The lateral variation of the illumination intensity is less than ± 0.05 sun, whereas the temperature during illumination is constant within a range of ± 2 °C. In order to deactivate the defect, the lifetime samples are illuminated at 0.5 suns for 30 min, at a reduced sample temperature of (36 ± 4) °C. Our preliminary investigations had shown that defect deactivation occurs under these conditions. Note that this temperature is caused by the halogen lamp illumination itself and measured on reference samples with a temperature probe (Testo AG). For selected samples, the degradation experiments are repeated several times, either at the same or each time at a different temperature during degradation.

We measure the effective lifetime (τ_{eff}) of the samples at (30 ± 2) °C by the photoconductance decay (PCD) method using a WCT-120 lifetime tester from Sinton Instruments (transient mode). If not stated otherwise, the lifetimes are reported at an excess carrier concentration of $\Delta n = 10^{15}$ cm^{-3}.

III. Experimental Results

A. Temperature-Dependent Degradation

Fig. 1 shows the degradation effects observed in the Cz-Si:Ga samples at temperatures ranging from 90 °C (black circles) to 140 °C (pink hexagons). Fig. 1(a) shows the measured effective lifetime τ_{eff} as a function of illumination time t at 1-sun illumination intensity. The corresponding evolution of the effective defect concentration $N_{\text{d}}^{*}(t)$ is plotted in Fig. 1(b). N_{d}^{*} is determined using the definition

$$N_{\text{d}}^{*}(t) = \frac{1}{\tau_{\text{d}}(t)} - \frac{1}{\tau_0} \tag{1}$$

with $\tau_{\text{d}}(t)$ being the lifetime after illumination for the time t and τ_0 being the lifetime before starting the illumination. The colors and symbols used in Fig. 1(a) match the ones in Fig. 1(b), whereas the dashed lines in Fig. 1(a) serve as guide to the eye, the lines in Fig. 1(b) are exponential rise-to-maximum fits of $N_{d}^{*}(t)$

$$N_{\text{d}}^{*}(t) = N_{\text{max}}^{*}\left(1 - e^{-R_{\text{deg}} \times t}\right) \tag{2}$$

with the maximum defect concentration N_{max}^{*} and the degradation rate constant R_{deg}. As clearly visible in Fig. 1, the extent of the lifetime degradation in Cz-Si:Ga shows a pronounced dependence on the applied temperature during illumination, whereas the degradation at 90 °C and 1 sun leads to a fully degraded state with $\tau_{\text{eff,d}} = 1300\,\mu$s at $\Delta n = 10^{15}$ cm^{-3} (initially $\tau_0 = 2300\,\mu$s), $\tau_{\text{eff,d}}$ is reduced to 500 μs, if the degradation is performed at 140 °C and 1 sun. As can be seen in Fig. 1(b), increasing the degradation temperature from 90 to 140 °C increases the maximum effective defect concentration N_{max}^{*} by a factor 5.

Surprisingly, we discovered that the observed temperature-dependent degradation effect in Cz-Si:Ga is fully reversible by illumination at reduced temperatures (e.g., at 0.5 suns and ∼36 °C for 30 min), which is shown in Fig. 2 for the effective defect concentration N_{d}^{*}. Note that a similar behavior at low temperatures has been reported for LeTID in mc-Si solar cells [22], [23] as well as in fired FZ-Si wafers [14]. We calculate the effective defect concentration $N_{\text{d}}^{*}(t)$ for the temporary defect deactivation using (1) and assuming the same τ_0 as for the defect activation before. A simple exponential decay function is fitted to the data shown in Fig. 2

$$N_{\text{d}}^{*}(t) = N_{\text{max}}^{*}\ e^{-R_{\text{de}} \times t}. \tag{3}$$

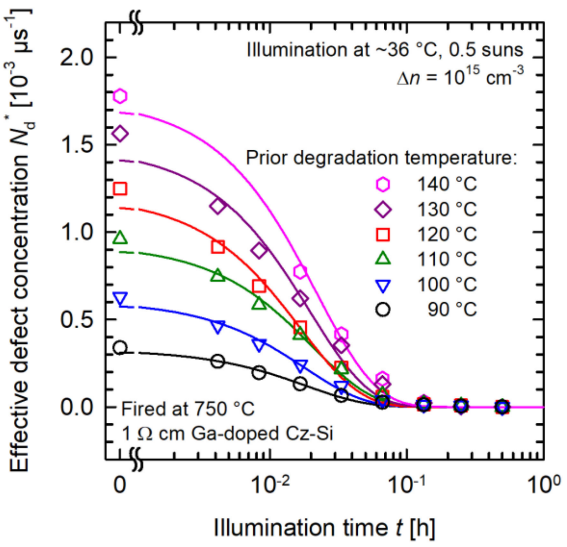

Fig. 2. Temporary deactivation of the Cz-Si:Ga degradation effect by illumination near room temperature (i.e., 0.5 suns, ~36 °C). Shown is the effective defect concentration $N_{\mathrm{d}}^{*}(\mathrm{t})$ (colors and symbols match the graphs in Fig. 1), the lines are exponential decay fits following (3).

The extracted deactivation rate constant R_{de} in Fig. 2 amounts to (52 ± 10) h^{-1} regardless of the degradation temperature applied before. The temporary deactivation is hence a very fast process, which is completely finished after 30 min.

Because of the fact that the defect activation and deactivation processes are fully reversible, all measured data shown in Fig. 1 have been obtained from the same lifetime sample by repeating the experiment at different temperatures, starting at the lowest temperature of 90 °C and increasing it for each repetition. After each complete degradation, the defect deactivation process applied in Fig. 2 has been used.

In order to verify the observed behavior on other samples, the dependence of the maximum defect concentration on the temperature has been confirmed on various samples. Furthermore, the complete and reversible deactivation has been confirmed by repeated activation/deactivation cycles on the same samples under constant degradation conditions.

Interestingly, we observe a qualitatively similar degradation behavior on our FZ-Si:B wafers as observed on our Cz-Si:Ga samples. Fig. 3 shows the degradation observed in our FZ-Si:B samples at temperatures ranging from 70 °C (black circles) to 120 °C (pink hexagons) at 1-sun illumination intensity. Fig. 3(a) shows the effective lifetime τ_{eff} as a function of illumination time t. The corresponding evolution of the effective defect concentration $N_{\mathrm{d}}^{*}(t)$ is plotted in Fig. 3(b), whereas degradation at 70 °C and 1 sun leads to a fully degraded state with $\tau_{\mathrm{eff,d}} = 4000\ \mu\mathrm{s}$ at $\Delta n = 10^{15}\ \mathrm{cm}^{-3}$ (initially $\tau_0 = 4300\ \mu\mathrm{s}$), $\tau_{\mathrm{eff,d}}$ is reduced to 3200 μs, if the degradation is performed at 100 °C and 1 sun. In contrast to the results on Cz-Si:Ga in Fig. 1, the maximum defect concentration N_{max}^{*} for FZ-Si:B in Fig. 3(b) reaches a maximum at a temperature of 100 °C and decreases for larger temperatures. This can be attributed to the onset of the defect deactivation under prolonged illumination, resulting in parallel degradation and regeneration of the effective lifetime (see also Section III-D). Since activation and deactivation of the defect are parallel processes, this effect leads to reduced N_{max}^{*} values for temperatures larger than 100 °C in the case of FZ-Si:B. We would hence expect the same effect for Cz-Si:Ga as well, but occurring at higher temperatures (>140 °C).

Importantly, the deactivation (regeneration) under prolonged illumination at elevated temperatures should not to be confused with the deactivation by illumination at low temperatures (e.g., 0.5 suns at ~36 °C, see Figs. 2 and 4). The deactivation close to room temperature is merely a temporary (nonpermanent) effect, whereas under prolonged illumination at elevated temperatures a permanent deactivation is achievable (see Section III-D).

The temporary defect deactivation at low temperatures on FZ-Si:B is shown in Fig. 4. The deactivation rate constant R_{de} calculated using (3) amounts to (74 ± 9) h^{-1}, which is even faster than on Cz-Si:Ga ($R_{\mathrm{de}} = (52 \pm 10)\ \mathrm{h}^{-1}$).

The maximum effective defect concentration N_{max}^{*} follows a linear correlation, if plotted versus the illumination temperature ϑ at constant illumination intensity. This is shown in Fig. 5 for an illumination intensity of 1 sun, whereas in case of Cz-Si:Ga the complete dataset (between 90 and 140 °C) can be fitted using a linear function (Fig. 5, black circles), only the limited temperature range from 70 to 100 °C follows a linear correlation for FZ-Si:B (Fig. 5, red squares). This can be attributed to the aforementioned onset of the permanent deactivation at higher temperatures. The lines in Fig. 5 show fits of the linear function

$$N_{\mathrm{max}}^{*} = a \times \vartheta + b \tag{4}$$

to the measured data. It is obvious from Fig. 5 that the slopes a differ by a factor ~10 [$a_{\mathrm{Cz:Ga}} = (28 \pm 1)\ \times 10^{-6}/(^{\circ}\mathrm{C} \times \mu\mathrm{s})$ and $a_{\mathrm{FZ:B}} = (2.3 \pm 0.1)\ \times 10^{-6}/(^{\circ}\mathrm{C} \times \mu\mathrm{s})$] for the two materials. The temperature where no degradation should be observable at all (i.e., the intercept with the temperature axis) is determined to be 78 °C for Cz-Si:Ga and 65 °C for FZ-Si:B. Experiments at 80 °C for Cz-Si:Ga, however, revealed that a degradation is still observable, but the maximum defect concentration is minimal ($N_{\mathrm{max}}^{*} < 0.2 \times 10^{-3} \mu\mathrm{s}^{-1}$).

Please note that N_{max}^{*} in FZ-Si:B is significantly smaller than on the Cz-Si:Ga wafers (by a factor ~6 at 90 °C, as the comparison between black circles and red squares in Fig. 5 reveals), whereas the actual peak temperatures in the firing furnace showed a difference of ~40 °C for the two different materials under examination (because of different optical properties, the FZ-Si:B wafers are shiny-etched), it is more likely that the significantly reduced amount of impurities in FZ-Si:B is responsible for the observed differences. However, a certain influence of the firing peak temperature cannot be excluded as well.

Reference measurements on nonfired samples revealed no significant degradation. In Fig. 6, the initial and degraded injection-dependent lifetime data of both a fired and a nonfired lifetime sample illuminated at 100 °C and 1 sun are depicted, although nonfired Cz-Si:Ga shows indeed a very slow degradation, resulting in a reduction of the lifetime from 1600 to 1400 μs at $\Delta n = 10^{15}\ \mathrm{cm}^{-3}$ within 4 h (Fig. 6, red squares), the degradation is much less severe than for fired Cz-Si:Ga wafers under the same conditions (Fig. 6, black circles). In addition, no lifetime recovery at illumination near room temperature is

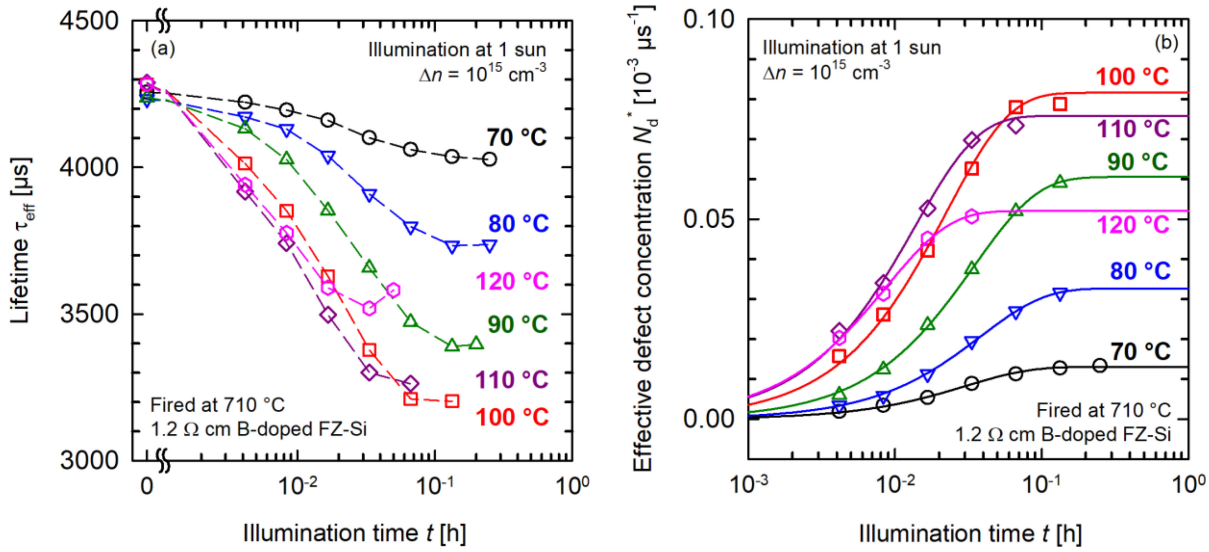

Fig. 3. Lifetime degradation of FZ-Si:B illuminated at 1 sun at temperatures ranging from 70 to 120 °C. (a) Effective lifetime $\tau_{\rm eff}$ at $\Delta n = 10^{15}$ cm^{-3}, as a function of illumination time t. The dotted lines serve as guide to the eye. (b) Corresponding effective defect concentration $N_{\rm d}^*(t)$ (colors and symbols match the graphs in (a)). The lines are exponential rise-to-maximum fits of the measurement data calculated by using (2).

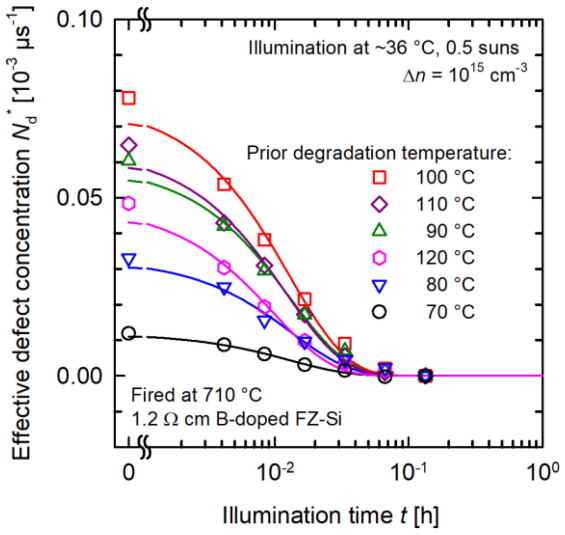

Fig. 4. Temporary deactivation of the FZ-Si:B degradation effect by illumination near room temperature (i.e., 0.5 suns, ~36 °C). Shown is the effective defect concentration $N_{\rm d}^*(t)$ (colors and symbols match the graphs in Fig. 3), the lines are exponential decay fits following (3).

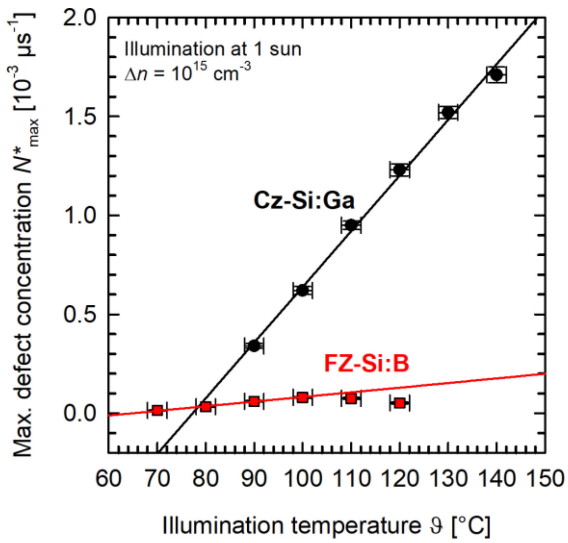

Fig. 5. Maximum defect concentration $\rm N^*_{max}$ as a function of the illumination temperature ϑ for Cz-Si:Ga (black circles) and FZ-Si:B (red squares). The lines are linear fits for either the complete set of data (Cz-Si:Ga) or for the data measured in the temperature range 70 – 100 °C (FZ-Si:B).

observed afterwards on nonfired Cz-Si:Ga for 20 h. This makes it very unlikely that the observed slight degradation effect has the same physical origin as the one reported on fired Cz-Si:Ga wafers. Furthermore, the lifetime of nonfired FZ-Si:B remains completely stable at 3200 μs under the same conditions. Note that dark anneal experiments with fired samples at the same temperature of 100 °C showed no degradation either within 1 h.

We conclude that charge carrier injection is necessary to activate the temperature-dependent degradation effect, which is triggered by the fast-firing step. The participation of hydrogen in the defect physics is therefore likely. It diffuses from the hydrogen-rich passivation layers into the silicon bulk during fast firing [14], [24]–[26].

B. Activation Energy

We determine the activation energy $E_{\rm A}$ of the observed temperature-dependent degradation effect by fitting the temperature dependence of the degradation rate constant $R_{\rm deg}$ using the Arrhenius law

$$R_{\rm deg}\ (T) = k_0\ \times \exp\left(-\frac{E_{\rm A}}{k_{\rm B}T}\right) \tag{5}$$

with a temperature-independent prefactor k_0, the Boltzmann constant $k_{\rm B}$, and the absolute temperature T. The corresponding plots for both Cz-Si:Ga (black circles) and FZ-Si:B (red squares) are shown in Fig. 7.

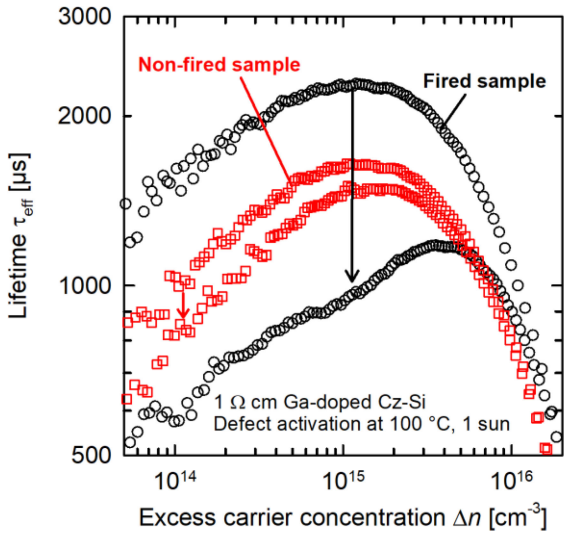

Fig. 6. Injection-dependent lifetimes for deactivated (upper curve) and activated (lower curve) defect in Cz-Si:Ga at 100 °C and 1-sun light intensity. Shown are a fired (black circles) and a non-fired (red squares) sample.

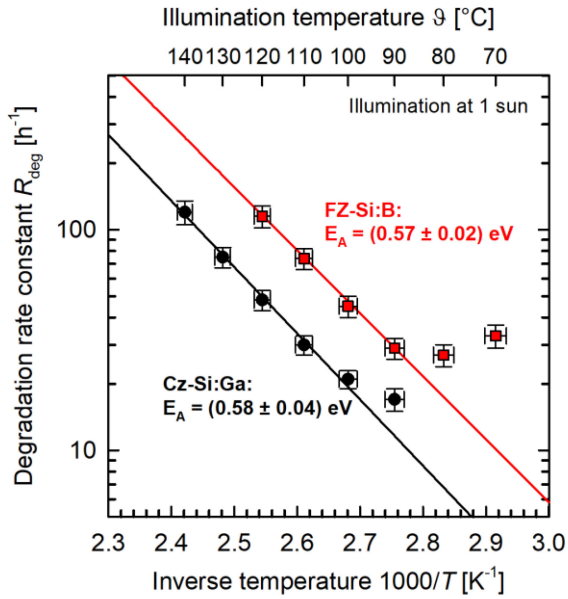

Fig. 7. Arrhenius plot of the degradation rates over the inverse temperature $1/T$ for Cz-Si:Ga (black circles) and FZ-Si:B (red squares). The lines are Arrhenius fits following (5) of the complete set of temperatures ranging from 90 to 140 °C for Cz-Si:Ga and a limited set of temperatures ranging from 90 to 120 °C for FZ-Si:B.

Note that there are significant deviations from the Arrhenius law visible in FZ-Si:B for the low temperatures of 70 and 80 °C. A possible reason are the very few and fixed measurement intervals chosen for the experiment, which leads to a high dependence on individual measured values, especially for the low temperatures where the magnitude of degradation is quite low. It is, however, also possible that the degradation rate constant R_{deg} indeed saturates because of the detailed defect physics, which is currently unknown. At the moment, we fit only the rate constants in the temperature ranges between 90 and 120 °C by the Arrhenius law for the FZ-Si:B lifetime sample. The deviations from the Arrhenius law of the Cz-Si:Ga samples are minimal, which is why we use the complete dataset in the temperature range 90–140 °C.

We obtain activation energies of $E_{\mathrm{A,Cz:Ga}} = (0.58 \pm 0.04)$ eV and $E_{\mathrm{A,FZ:B}} = (0.57 \pm 0.02)$ eV. These values are identical within the respective measurement uncertainty ranges. However, the temperature independent prefactor k_0 differs by a factor of almost 2: $k_{0,\mathrm{Cz}} = (1.37 \pm 0.07) \times 10^9\,\mathrm{h}^{-1}$ for Cz-Si:Ga and $k_{0,\mathrm{FZ}} = (2.09 \pm 0.07) \times 10^9\,\mathrm{h}^{-1}$ for FZ-Si:B.

To determine the uncertainty for the degradation rate constants R_{deg} in Fig. 7, we generate an ensemble of random deviations from the measured lifetime data using a normal distribution. We assume a standard deviation (1 σ) of 2% for the original lifetime measurements shown in the Figs. 1(a) and 3(a). Thereby, each lifetime measurement already represents an averaged value over five measurements using the WCT-120 built-in average tool. This assumption is in agreement with the general uncertainty of the lifetime measurement via PCD reported by McIntosh and Sinton [27]. Furthermore, we assume a standard deviation for each illumination interval of 2 s to determine ΔR_{deg}. We calculate the uncertainty ranges for the activation energy E_{A} following the publication by Reed [28] taking into account both the uncertainty for the degradation rate constant R_{deg} and the temperature T (i.e., 2 K).

For comparison, Bredemeier *et al.* determined E_{A} for the double-exponential LeTID effect on B-doped mc-Si to be $E_{\mathrm{A,\,LeTID}} = (0.94 \pm 0.06)$ eV [29]. Please note, that Bredemeier *et al.* determined E_{A} at an illumination intensity of 0.5 suns instead of 1 sun. This, however, should have no impact on the value of the activation energy. Vargas *et al.* determined $E_{\mathrm{A,LeTID}}$ to be (1.08 ± 0.05) eV [30] and Graf et al. determined the activation energy of a degradation effect observed in fired FZ-Si to be $E_{\mathrm{A,\,FZ:B}} = (0.8 \pm 0.12)$ eV [13].

Thus, the activation energy determined in this contribution is significantly lower than activation energies reported for LeTID in the literature. This suggests that the detailed defect reactions leading to the degradation are different in the samples examined in this study.

C. Illumination Intensity Dependence

In this section, we examine the impact of the illumination intensity I_{ill} on the degradation dynamics at a fixed degradation temperature of 100 °C, while I_{ill} is varied between 0.1 and 1 suns. Fig. 8 shows both the maximum defect concentrations N^*_{max} [Fig. 8(a)] and the degradation rate constants R_{deg} [Fig. 8(b)].

As clearly visible in Fig. 8(a), for applied illumination intensities I_{ill} above 0.25 suns, N^*_{max} does not depend on the intensity I_{ill}. The increased N^*_{max} at $I_{\mathrm{ill}} = 0.1$ suns in the case of the Cz-Si:Ga sample was not observed on the FZ-Si:B material. This, however, could be related to the higher effective lifetime in FZ-Si:B in general, which leads to a higher excess carrier concentration Δn than in Cz-Si:Ga under the same illumination conditions. A shift of the increasing N^*_{max} in FZ-Si:B to lower intensities than 0.1 suns is therefore possible. Another explanation could be an impact of the permanent deactivation of the defect at elevated temperatures for higher illumination intensities. A delayed onset at lower illumination intensities could explain the higher maximum defect concentration N^*_{max} value, since both the activation and deactivation of the defect

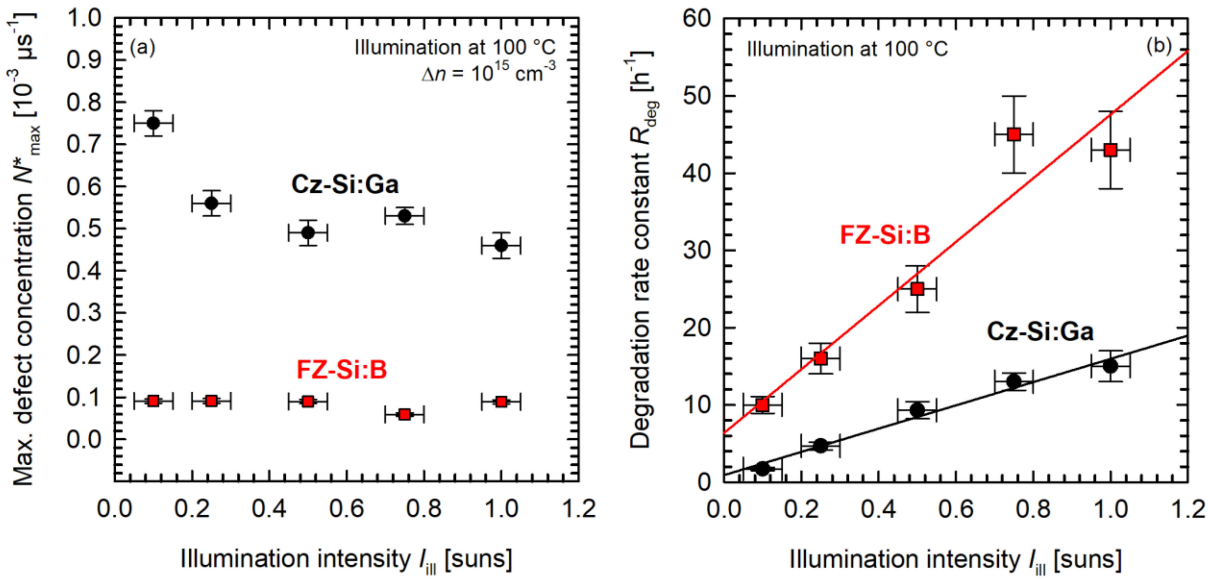

Fig. 8. (a) Maximum defect concentration $\mathbf{N^*_{max}}$ and (b) degradation rate R_{deg} plotted versus the illumination intensity I_{ill} for Cz-Si:Ga (black circles) and FZ-Si:B (red squares). The temperature applied during the degradation is 100 °C for both sample types. The data in (b) are fitted using a linear regression.

are most likely independent and parallel processes. However, a general dependence of the maximum defect concentration on the illumination intensity is not observed.

As can be seen in Fig. 8(b), the degradation rate constant R_{deg} increases linearly with the illumination intensity I_{ill} between 0.1 and 1 suns. The solid lines in Fig. 8(b) shows linear fits using the equation

$$R_{\mathrm{deg}} = a \times I_{ill} + b. \tag{6}$$

The slope a is determined to be $a_{\mathrm{Cz:Ga}} = (15 \pm 2)$ $\mathrm{h^{-1}\ suns^{-1}}$ and $a_{\mathrm{FZ:B}} = (41 \pm 8)$ $\mathrm{h^{-1}\ suns^{-1}}$. The y-intercept is $b_{\mathrm{Cz:Ga}} = (0.9 \pm 0.8)$ $\mathrm{h^{-1}}$ and $b_{\mathrm{FZ:B}} = (6 \pm 5.)$ $\mathrm{h^{-1}}$. As we mentioned briefly at the end of Section III-A, carrier injection is a necessary requirement for the defect activation. Naturally, the intercept with the *y*-axis, *b,* should therefore be zero. However, currently we have not collected any data at illumination intensities lower than 0.1 suns, where possible deviations from the linear correlation shown in Fig. 8(b) could be visible. For the moment, we kept *b* hence fixed at nonzero values.

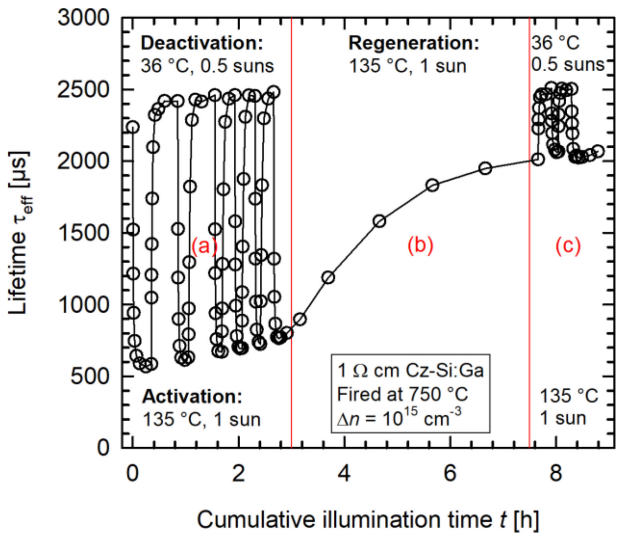

Fig. 9. Repeated activation/deactivation cycles of the degradation effect in Cz-Si:Ga interrupted by a permanent deactivation step (Regeneration) under prolonged illumination at elevated temperature (i.e., 135 °C).

D. Permanent Deactivation (Lifetime Regeneration)

Apart from the aforementioned temporary (nonpermanent) deactivation of the responsible defect, our experiments show that also a permanent deactivation is possible for both Cz-Si:Ga and FZ-Si:B (the latter not shown here), whereas the temporary deactivation requires illumination near room temperature (e.g., 0.5 suns, ∼36 °C, see Figs. 2 and 4), the permanent defect deactivation requires a prolonged illumination at high-intensity and elevated temperatures (e.g., 1 sun, 135 °C). In Fig. 9, several defect activation and (temporary) deactivation cycles are shown for a Cz-Si:Ga sample interrupted by a permanent deactivation step (leading to a lifetime regeneration). First, the lifetime is cycled between the active and in-active defect state six times, by changing the conditions the samples are exposed to between 135 °C and 1 sun and 36 °C and 0.5 suns [Fig. 9(a)]. After each defect activation at elevated temperature, the exposure to illumination at lower temperature leads to a complete deactivation of the defect. The sample is then exposed for approximately 4 h to illumination at 135 °C, which leads to a slow recovery of the lifetime [regeneration, Fig. 9(b)]. A subsequent cycling between both illumination conditions shows that the minimum lifetime now equals the lifetime value after prolonged illumination at

135 °C [Fig. 9(c)]. This observation clearly supports that a permanent defect deactivation (leading to a lifetime regeneration) is possible.

Please note, however, that the prolonged illumination at 135 °C in Fig. 9(b) apparently does not lead to a complete permanent defect deactivation. A temperature dependence of the permanent deactivation is a possible explanation. However, at this point we have not collected enough data on the regeneration behavior to state this as a fact.

IV. Conclusion

In this contribution, we have performed a series of carrier lifetime experiments at elevated temperatures between 70 and 140 °C and illumination intensities ranging from 0.1 to 1 sun. We observed very similar temperature-dependent degradation effects in Cz-Si:Ga and FZ-Si:B wafers. This is particularly interesting since Cz-Si:Ga is expected to become the most commonly used material in industrial solar cell production in the near future.

The degradation in both cases was because of illumination, and fast firing of the samples was required to trigger the degradation, whereas the extent of degradation is strongly dependent on the applied temperature—with higher temperatures leading to a stronger degradation—we observed no dependence of the degradation extent on the illumination intensity. Additionally, we determined the activation energy of the degradation processes in both materials to be practically identical at $E_{\mathrm{A}} = (0.58 \pm 0.04)$ eV. This suggests that the degradation mechanism observed in this contribution is different to the well-known LeTID effect observed on mc-Si materials, where significantly higher activation energies have been reported in the literature [29], [30].

We hence conclude that the detailed defect physics is different in fired Cz-Si:Ga and FZ-Si:B compared with LeTID, although hydrogen is probably involved in all these degradation effects.

We found that the defect responsible for the degradation effect can be deactivated temporarily by a simple illumination near room temperature (e.g., at 0.5 suns and ∼36 °C). However, a permanent deactivation can also be achieved when prolonged illumination at elevated temperatures and light intensities around 1 sun are applied.

References

[1] J. Schmidt, A. G. Aberle, and R. Hezel, "Investigation of carrier lifetime instabilities in CZ grown silicon," in *Proc. Conf. Rec. 26th IEEE Photovoltaic Specialists Conf.,* Anaheim, CA, USA, 1997, pp. 13–18.

[2] S. W. Glunz, S. Rein, W. Warta, J. Knobloch, and W. Wettling, "On the degradation of Cz-silicon solar cells,"in *Proc. 2nd World Conf. Photovoltaic Sol. Energy Convers.,* Vienna, Austria, 1998, pp. 1343–1346.

[3] T. Saitoh *et al.*, "Light degradation and control of low-resistivity Cz-Si solar cells—-An international joint research," in *Proc. Tech. Dig. 11th Int. Photovoltaic Sci. Eng. Conf.*, Sapporo, Japan, 1999, pp. 553–556.

[4] J. Schmidt and K. Bothe, "Structure and transformation of the metastable boron- and oxygen-related defect center in crystalline silicon," *Phys. Rev. B*, vol. 69, no. 2, 2004, Art. no. 24107.

[5] K. Ramspeck *et al.*, "Light induced degradation of rear passivated mc-Si solar cells," in *Proc. 27th Eur. Photovoltaic Sol. Energy Conf. Exhib.*, Frankfurt, Germany, 2012, pp. 861–865.

[6] K. Krauss, F. Fertig, D. Menzel, and S. Rein, "Light-induced degradation of silicon solar cells with aluminiumoxide passivated rear side," *Energy Procedia*, vol. 77, pp. 599–606, 2015.

[7] F. Kersten *et al.*, "System performance loss due to LeTID," *Energy Procedia*, vol. 124, pp. 540–546, 2017.

[8] D. Bredemeier, D. C. Walter, and J. Schmidt, "Lifetime degradation in multicrystalline silicon under illumination at elevated temperature: Indications for the involvement of hydrogen," *AIP Conf. Proc.*, Lausanne, Switzerland, vol. 1999, no. 1, 2018, Art. no. 130001.

[9] C. E. Chan *et al.*, "Rapid stabilization of high-performance multicrystalline P-type silicon PERC cells," *IEEE J. Photovolt.*, vol. 6, no. 6, pp. 1473–1479, Nov. 2016.

[10] K. Nakayashiki *et al.*, "Engineering solutions and root-cause analysis for light-induced degradation in p-type multicrystalline silicon PERC modules," *IEEE J. Photovolt.*, vol. 6, no. 4, pp. 860–868, Jul. 2016.

[11] F. Fertig *et al.*, "Mass production of p-type Cz silicon solar cells approaching average stable conversion efficiencies of 22%," *Energy Procedia*, vol. 124, pp. 338–345, 2017.

[12] D. Chen *et al.*, "Evidence of an identical firing-activated carrier-induced defect in monocrystalline and multicrystalline silicon," *Sol. Energy Mater. Sol. Cells*, vol. 172, pp. 293–300, 2017.

[13] A. Graf, A. Herguth, and G. Hahn, "Determination of BO-LID and LeTID related activation energies in Cz-Si and FZ-Si using constant injection conditions," *AIP Conf. Proc.,* Leuven, Belgium, vol. 2147, no. 1, 2019, Art. no. 140003.

[14] T. Niewelt *et al.*, "Understanding the light-induced degradation at elevated temperatures: Similarities between multicrystalline and floatzone p-type silicon," *Prog. Photovolt. Res. Appl.*, no. 8, pp. 1–10, 2017.

[15] D. Sperber, A. Herguth, and G. Hahn, "A 3-state defect model for light-induced degradation in boron-doped float-zone silicon," *Phys. Status Solidi RRL*, vol. 11, no. 3, 2017, Art. no. 1600408.

[16] D. Chen *et al.*, "Hydrogen induced degradation: A possible mechanism for light- and elevated temperature- induced degradation in n-type silicon," *Sol. Energy Mater. Sol. Cells*, vol. 185, pp. 174–182, 2018.

[17] N. E. Grant *et al.*, "Gallium-Doped silicon for high-efficiency commercial passivated emitter and rear solar cells," *Sol. RRL*, vol. 7, 2021, Art. no. 2000754.

[18] N. E. Grant *et al.*, "Lifetime instabilities in gallium doped monocrystalline PERC silicon solar cells," *Sol. Energy Mater. Sol. Cells*, vol. 206, 2020, Art. no. 110299.

[19] W. Kwapil, J. Dalke, T. Niewelt, and M. C. Schubert, "LeTID and (extended) BO-related degradation and regeneration in B- and Ga-doped monocrystalline silicon during dark and illuminated anneals," in *Proc. 37th Eur. Photovoltaic Sol. Energy Conf. Exhib.*, Munich, Germany, pp. 152–155, 2020.

[20] H. C. Sio, D. Kang, X. Zhang, J. Yang, J. Jin, and D. Macdonald, "The role of dark annealing in light and elevated temperature induced degradation in p-type mono-like silicon," *IEEE J. Photovolt.*, vol. 10, no. 4, pp. 992–1000, Jul. 2020.

[21] M. Winter, L. Helmich, D. C. Walter, and J. Schmidt, "Firing-Triggered LID (FT-LID) of the carrier lifetime in Cz-Si," in *Proc. 37th Eur. Photovoltaic Sol. Energy Conf.*, Munich, Germany, 2020, pp. 462–467.

[22] F. Kersten *et al.*, "A new light induced volume degradation effect of mc-Si solar cells and modules," in *Proc. 31th Eur. Photovoltaic Sol. Energy Conf. Exhib.*, Hamburg, Germany, 2015, pp. 1830–1834.

[23] W. Kwapil, J. Schon, T. Niewelt, and M. C. Schubert, "Temporary recovery of the defect responsible for light- and elevated temperature-induced degradation: Insights into the physical mechanisms behind LeTID," *IEEE J. Photovolt.*, vol. 10, no. 6, pp. 1591–1603, Nov. 2020.

[24] D. Bredemeier, D. C. Walter, R. Heller, and J. Schmidt, "Impact of hydrogen-rich silicon nitride material properties on light-induced lifetime degradation in multicrystalline silicon," *Phys. Status Solidi RRL*, vol. 31, 2019, Art. no. 1900201.

[25] F. Kersten, J. Heitmann, and J. W. Müller, "Influence of Al2O3 and sinx passivation layers on LeTID," *Energy Procedia*, vol. 92, pp. 828–832, 2016.

[26] C. Vargas *et al.*, "Carrier-Induced degradation in multicrystalline silicon: Dependence on the silicon nitride passivation layer and hydrogen released during firing," *IEEE J. Photovolt.*, vol. 8, no. 2, pp. 413–420, Mar. 2018.

[27] K. R. McIntosh and R. A. Sinton, "Uncertainty in photoconductance lifetime measurements that use an inductive-coil detector," in *Proc. 23rd Eur. Photovoltaic Sol. Energy Conf. Exhib.*, Valencia, Spain, 2008, pp. 77–82.

[28] B. C. Reed, "Linear least-squares fits with errors in both coordinates," *Amer. J. Phys.*, vol. 57, no. 7, pp. 642–646, 1989.

[29] D. Bredemeier, D. Walter, and J. Schmidt, "Light-induced lifetime degradation in high-performance multicrystalline silicon: Detailed kinetics of the defect activation: 6th international conference on silicon photovoltaics, SiliconPV 2016," *Sol. Energy Mater. Sol. Cells*, vol. 173, pp. 2–5, 2017.

[30] C. Vargas, G. Coletti, C. Chan, D. Payne, and Z. Hameiri, "On the impact of dark annealing and room temperature illumination on p-type multicrystalline silicon wafers," *Sol. Energy Mater. Sol. Cells*, vol. 189, pp. 166–174, 2019.